Introduction of a *lacZ* reporter gene into the mouse *int-2* locus by homologous recombination

(gene targeting/embryo-derived stem cells/mouse *hprt* gene)

SUZANNE L. MANSOUR, KIRK R. THOMAS, CHUXIA DENG, AND MARIO R. CAPECCHI

Howard Hughes Medical Institute, Department of Biology, University of Utah, Salt Lake City, UT 84112

ABSTRACT   We demonstrate that the frequency of gene targeting is unaffected by the length of nonhomologous DNA transferred to a target chromosomal sequence. A result of this finding is that a much wider spectrum of designed genomic alterations is now feasible. As a first application, we inserted a 5.4-kilobase cassette of nonhomologous DNA into the *int-2* locus in mouse embryo-derived stem cells by gene targeting. The inserted DNA contained a *lacZ* gene positioned to create an in-frame fusion with the *int-2* protein-coding region. Upon differentiation of these cells to embryoid bodies, the *int-2–lacZ* fusion faithfully reproduced the expression pattern of *int-2* RNA. This ability to target reporter genes, such as *lacZ*, to specific mouse loci, combined with the ability to move the tagged gene into different mutant backgrounds, may provide an ideal approach for analyzing interactions among genes that participate in a developmental network.

Homologous recombination between an exogenously introduced DNA molecule and its endogenous chromosomal counterpart provides a means to transfer specific sequence modifications, created *in vitro*, into the genome of an intact cell. Furthermore, if the recipient cell is a pluripotent, mouse embryo-derived stem (ES) cell, then it is possible to transfer that modified gene to the genome of a living mouse. In this way, the effects of designed genome alterations can be monitored in the context of the entire mammalian developmental program (for reviews, see refs. 1–3).

It is commonly believed that the frequency of gene targeting events in mammalian cells is inversely proportional to the length of nonhomologous DNA sequences that are transferred to the chromosomal target (4–7). This belief is based in part on the observation that in cultured mammalian cells, the frequency of intrachromosomal gene conversion is inversely proportional to the length of nonhomologous DNA converted in the recipient DNA sequence (8). However, the recombination substrates that participate in gene targeting and in intrachromosomal gene conversion are different, and therefore the above assumption warranted direct investigation.

In this paper we demonstrate that the frequency of gene targeting at the mouse hypoxanthine phosphoribosyltransferase (*hprt*) locus is insensitive to the length of nonhomologous DNA transferred to the target chromosomal sequence. This finding vastly increases the spectrum of potential genomic alterations that can be generated by gene targeting. As an initial test of this unexpected observation, we introduced 5.4 kilobases (kb) of nonhomologous DNA containing the genes which encode β-galactosidase (β-gal) and neomycin resistance (neo^r) into one of the endogenous *int-2* alleles in an ES cell line.

int-2 is a protooncogene identified by its activation in mouse mammary tumors due to the nearby insertion of mouse mammary tumor virus DNA (9, 10). *int-2* is a member of the fibroblast growth factor gene family (11), and analysis of the pattern of *int-2* expression suggests several potential roles for this gene in cell–cell interactions during normal mouse development (12, 13). ES cells provide an *in vitro* model for some of the early events in mammalian development, and this property facilitates the analysis of certain aspects of the *int-2* expression pattern. Upon *in vitro* differentiation of ES cells, *int-2* mRNAs are induced dramatically and are restricted to a subpopulation of extraembryonic-like endodermal cells (12, 14). We show here that the *int-2–lacZ* fusion faithfully displays this expected *int-2* expression pattern.

MATERIALS AND METHODS

Vector Construction. The *hprt* vectors were constructed by starting with a 9.1-kb fragment of *hprt* (4) that extends from a *Bgl* II site in intron 5 to a *Bgl* II site 3′ of *hprt* coding sequences. To create pHPT^{+8}, an 8-base-pair (bp) *Xho* I linker was inserted into the *Sca* I site in exon 8. pHPT^{+1k} and pHPT$^{+3.4k}$ were created by inserting a 1-kb fragment from pMC1-NEO (4) and a 3.4-kb fragment from pC4βgal (15), respectively, into the *Xho* I linker in pHPT^{+8}.

The *int-2–lacZ* replacement vector, pINT-2-LACZN/TK, was constructed by starting with pINT-2-NpA, which contains a 10-kb *Eco*RI fragment of *int-2* genomic DNA (10) disrupted at the *Apa* I site in exon 1b by the insertion of the polyadenylylation signal-containing neo^r gene from pMC1-NEOpA. A DNA fragment from pC4βgal (15) that contains the *Escherichia coli lacZ* gene, missing the first seven codons, and followed by the simian virus 40 small t splice and early polyadenylylation signals, was inserted into pINT-2-NpA within exon 1b such that the reading frame between the first 21 *int-2* codons and the *lacZ* sequences was preserved, creating pINT-2-LACZN. The herpes simplex virus thymidine kinase (HSV-tk) gene (16) was inserted into pINT-2-LACZN on the 5′ side of the *int-2* sequences, creating pINT-2-LACZN/TK.

Electroporation and Isolation of Cell Lines. Linearized plasmid DNAs were introduced by electroporation into the ES cells as described previously (4). Isolation of 6-thioguanine-resistant (6-TG^r) and G418^r plus gancyclovir-resistant (GANC^r) cell lines was as described previously (4, 16) except for the following changes in the isolation of 6-TG^r cell lines. After electroporation of ES cells with the *hprt* targeting vectors, 2 × 10^4 ES cells were plated on 100-mm culture plates that contained feeder STO cells in nonselective medium. After 4 days of incubation, ⅕ of the cells on a single

Abbreviations: ES, embryo-derived stem; β-gal, β-galactosidase; HSV-tk, herpes simplex virus thymidine kinase; GANC, gancyclovir; 6-TG, 6-thioguanine; ^r, resistant; FDG, fluorescein β-D-galactopyranoside.

plate were transferred to a fresh feeder layer in growth medium that contained 6-TG at 1 μg/ml. Three days later, the cells from a single plate were again transferred to a new feeder layer in 6-TG medium. Under these conditions, at least 33% of the resulting plates had no 6-TG^r colonies, consistent with the Poisson prediction of a single mutational event per plate.

Embryoid Body Formation and Fluorescence Imaging of β-gal Activity and SPARC Antigen. Embryoid body formation was initiated according to Martin *et al.* (17). Four days after the initial cell clumps were put into suspension culture, the embryoid bodies were assayed *in vivo* for β-gal activity with fluorescein β-D-galactopyranoside (FDG) as the substrate. Reagents for the assay were purchased from Molecular Probes. The assay was performed as described by the supplier and by Nolan *et al.* (18). The embryoid bodies were observed in microconcavity slides by using a Bio-Rad confocal laser scanning microscope equipped for simultaneous phase-contrast and fluorescence observation (fluorescein filters). The microscope stage was cooled to 4°C to prevent leakage of fluorescein from cells.

SPARC antigen (19) was detected by using a whole-mount indirect immunofluorescence protocol (C. Davis, D. Holmyard, K. Millen, and A. Joyner, personal communication) based on refs. 20 and 33. The primary rabbit anti-SPARC serum (a gift of B. Hogan) was used at a 1:200 dilution. The secondary Texas red-labeled donkey anti-rabbit IgG (Jackson ImmunoResearch) was used at a 1:100 dilution. The stained embryoid bodies were observed by using the confocal microscope equipped with rhodamine filters.

RESULTS

Disruption of the *hprt* Gene with Inserts of Different Size. To assess the effect of sequence heterology on the frequency of gene targeting, insertions of various lengths were targeted to the X chromosome-linked *hprt* locus in male ES cells. The targeting vectors illustrated in Fig. 1 each contained a 9.1-kb fragment of the *hprt* gene that was disrupted by heterologous DNA inserts of 8 bp, 1 kb, or 3.4 kb located within the eighth exon. Homologous recombination between the targeting vectors and the endogenous gene would disrupt the *hprt* coding sequences, rendering the cells *hprt*$^-$ and thus resistant to the purine analog 6-TG. The linearized vector DNAs were introduced separately into ES cells by electroporation. These cells were then subjected to selection in medium containing 6-TG. We found the frequency of targeted disruption of *hprt* to be the same irrespective of the length of the heterologous
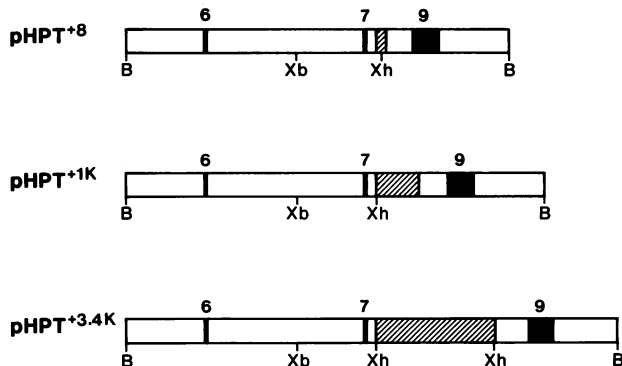

FIG. 1. *hprt* targeting vectors. The closed boxes represent *hprt* exons, numbered according to the map of Melton *et al.* (21). Open boxes represent introns and 3' noncoding sequences. The hatched boxes represent heterologous DNA inserted into the eighth exon of *hprt*. The lengths of the inserted DNAs in each vector are as follows: pHPT^{+8}, 8 bp; pHPT^{1k}, 1 kb; pHPT$^{3.4k}$, 3.4 kb. Restriction endonuclease sites: B, *Bgl* II; Xb, *Xba* I; Xh, *Xho* I.

Table 1. Gene targeting into the *hprt* locus

Vector	No. cells surviving electroporation	6-TG^r colonies	Targeted *hprt*$^-$ colonies/ 6-TG^r colonies tested
pHPT^{+8}	1 × 10^6	15	6/12
pHPT^{+1k}	1 × 10^6	15	6/9
pHPT$^{+3.4k}$	1 × 10^6	15	9/15
pHPT3$^{+4.3k}$	1.4 × 10^6	12	6/12
pHPT3^{+12k}	2 × 10^6	28	15/28

Linearized DNAs were introduced into ES cells by electroporation. Aliquots of cells treated with *hprt* vectors were grown either in nonselective medium to assess the total number of cells surviving electroporation (approximately 50%) or in 6-TG-containing medium to select for *hprt*$^-$ cells. Targeting events were identified by Southern transfer analysis (see Fig. 2). pHPT^{+8}, pHPT^{+1k}, and pHPT$^{+3.4k}$ are *hprt* vectors that contain heterologous inserts in the eighth exon of 8 bp, 1 kb, and 3.4 kb, respectively (Fig. 1). pHPT3$^{+4.3k}$ and pHPT3^{+12k} are *hprt* vectors that contain heterologous inserts in the third exon of 4.3 kb and 12 kb, respectively (structures not shown).

DNA inserted into the endogenous gene (Table 1). In addition to this study of heterologous inserts in the eighth exon, we have also examined the effect of heterologous inserts of 4.3 kb and 12 kb in the third exon on the *hprt* targeting frequency. As can be seen from Table 1, comparable targeted disruption frequencies were also obtained with these *hprt* vectors.

DNA from each independent 6-TG^r colony was subjected to Southern blot hybridization analysis to determine whether resistance to 6-TG resulted from targeted disruption of the *hprt* gene or from spontaneous mutation. Approximately 50% of the 6-TG^r colonies arose as a result of targeted disruption of the *hprt* gene, regardless of which targeting vector was used. The remaining 6-TG^r colonies arose by spontaneous mutation of the *hprt* gene (Table 1). Even though the spontaneous mutation rate at the *hprt* locus is approximately 1/20th of the gene targeting rate, the spontaneous *hprt*$^-$ mutants accumulate during the selection protocol, whereas gene targeting events occur only over a short period following the introduction of the targeting vector into the ES cells (1). This accounts for the eventual accumulation of approximately equal numbers of targeted and spontaneous *hprt*$^-$ mutations in these experiments.

Southern blot hybridization analysis of the *hprt*$^-$ cell lines with targeted insertions in exon 8 is shown in Fig. 2. Digestion of the parental *hprt*$^+$ ES DNA with the enzyme *Xba* I generated an 8.4-kb fragment which hybridized to the *hprt* probe. Because the three targeted *hprt*$^-$ cell lines analyzed here contain insertions of DNA in the eighth exon, the length of this *Xba* I fragment increased by the length of the insertion [i.e., 8 bp (not discernible), 1 kb, and 3.4 kb]. The insertion mutations were also characterized by the presence of an *Xho* I site, not found in the eighth exon of the wild-type gene. The presence of this site was demonstrated by digestion of the mutant DNAs with the enzymes *Xho* I and *Xba* I, which generate a 1.8-kb fragment common to the *hprt*$^-$ cell lines (Fig. 2). A similar analysis of the cell lines derived by targeting with the vectors that contain insertions in exon 3 confirmed the presence of the expected disruption in each case (data not shown).

Insertion of a *lacZ* Reporter Gene into the *int-2* Locus. Fig. 3A illustrates the *int-2* targeting vector, pINT-2-LACZN/TK. This vector contains an *int-2–lacZ* fusion, along with the *neo*^{r} and HSV-tk genes. The *lacZ* coding sequences, excluding the first seven codons, were fused in-frame with *int-2* coding sequences. The downstream *neo*^{r} gene, in the presence of G418, provides a positive selection for insertion of the targeting vector sequences. Similarly, the HSV-tk gene, in the presence of GANC, provides a negative selection to reduce the number of transfected ES cells that contain
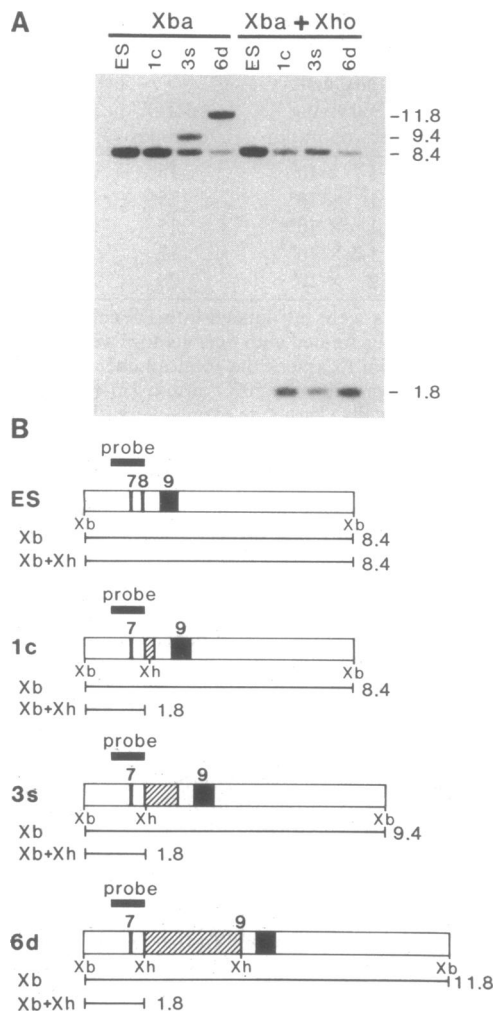
FIG. 2. Southern transfer analysis of gene targeting at the *hprt* locus. (*A*) DNA samples and enzymes with which they were digested are indicated above each lane. ES refers to DNA from the wild-type ES cell line; 1c, 3s, and 6d refer to DNAs from 6-TG^r cell lines targeted with pHPT^{+8}, pHPT^{+1k}, and pHPT$^{+3.4k}$, respectively. The probe is a 1-kb fragment of genomic *hprt* DNA (4, 16). The sizes of the hybridizing fragments are indicated to the right in kb. The 8.4-kb band seen in cell lines 1c, 3s, and 6d is from the STO-cell feeder layer upon which the ES cells are grown. (*B*) Schematic representation of the Southern transfer data. The 3' end of the *hprt* gene from each cell line is shown. Shading of the boxes is as in Fig. 1. Above each map are boxes showing the position of the probe fragment. Beneath each map are the restriction fragments that hybridize to the probe. Xb, *Xba* I; Xh, *Xho* I.

nontargeted insertions of the vector DNA (16). Homologous recombination between the *int-2* targeting vector and the endogenous *int-2* gene would precisely position the *lacZ* reporter gene within the *int-2* cis-regulatory environment and was therefore expected to place *lacZ* under *int-2* transcriptional and translational control (Fig. 3*B*).

The *int-2* targeting vector was linearized as shown and introduced into ES cells by electroporation, and the treated cells were grown in medium containing G418 and GANC. DNA from the doubly resistant cell lines was analyzed by restriction digestion and Southern blot hybridization, using enzymes and probes that distinguish random from homologous integration events. Of 89 cell lines examined, 9 were found to contain an insertion of the *lacZ* and *neo^r* DNAs in one of the two *int-2* alleles (Table 2).

Southern blot hybridization analysis of one of the targeted cell lines, 62-8K, is shown in Fig. 4. Parental ES DNA digested with *Hin*dIII and *Xho* I, or *Xmn* I alone, and probed
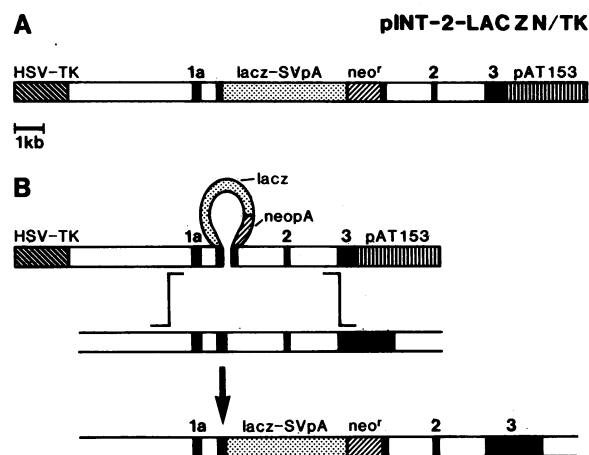

FIG. 3. *int-2–lacZ* targeting vector. (*A*) The closed boxes represent *int-2* exons (22, 23). Open boxes represent introns and noncoding sequences. The hatched boxes represent *neo^r* and HSV-tk DNAs as labeled, the stippled box denotes *lacZ* DNA, and the vertically striped box represents plasmid sequences. (*B*) Homologous recombination between the introduced vector DNA (pINT-2-LACZN/TK, upper line) and the endogenous *int-2* locus (middle line) gives rise to a mutant allele (lower line) in which *lacZ* sequences are fused in-frame with *int-2* coding sequences. Shadings are as described for *A*.

with flanking *int-2* sequences, not present in the targeting vector (probe A), reveals fragments of 11.2 kb and 6.2 kb, respectively. DNA from the mutant cell line, 62-8K, digested with the same enzymes, reveals fragments of the same size as those from the parental cell line. These are derived from the unmutagenized copy of the *int-2* gene. Probe A also detects new fragments of 6.7 kb (*Hin*dIII and *Xho* I) and 11.6 kb (*Xmn* I) derived from the mutated copy of *int-2*. The new fragments correspond in length to those predicted from homologous recombination between the targeting vector DNA and the endogenous *int-2* gene. As expected, these fragments both hybridize with the *neo^r* probe (probe B). In addition, the *lacZ* probe (probe C) hybridizes with a 10.2-kb fragment (*Hin*dIII and *Xho* I) and with an 11.6-kb fragment (*Xmn* I) in 62-8K DNA, confirming the presence of *lacZ* sequences at the expected site in the mutant allele.

Pattern of *int-2–lacZ* Expression in Differentiating Cultures of ES Cells. The earliest point in mouse embryogenesis at which *int-2* RNA has been detected is at 7.5 days in parietal endoderm, an extraembryonic tissue (12). A similar pattern of expression is observed *in vitro* when ES cells are induced to differentiate by growth in suspension culture. The resulting embryoid bodies contain two cell types; a ball of undiffer-

Table 2. Gene targeting into the *int-2* locus by pINT-2-LACZN/TK

Exp.	No. cells surviving electroporation	G418^r colonies	G418^r+GANC^r colonies	Targeted G418^r+GANC^r colonies/ G418^r+GANC^r colonies
1	5 × 10^6	5.2 × 10^4	46	5/46
2	5 × 10^6	4.9 × 10^4	43	4/43

Aliquots of cells treated with the *int-2* vector (Fig. 3*A*) were subjected to one of three growth conditions: nonselective medium to assess the total number of cells surviving electroporation (approximately 50%), G418 medium to assess the fraction of survivors transformed by the *lacZ–neo^r* vector, or G418 plus GANC medium to enrich for cells containing a targeted disruption of the *int-2* gene. Among the G418^r+GANC^r colonies, targeting events were identified by Southern transfer analysis (see Fig. 4).
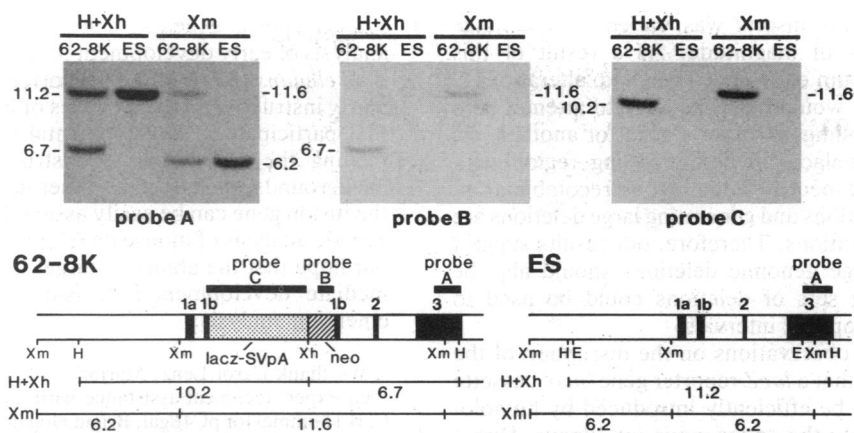
FIG. 4. Southern blot hybridization analysis of gene targeting at the *int-2* locus. (*Upper*) DNA samples and the enzymes with which they were digested are indicated above each lane (targeted cell line, 62-8K; parental cell line, ES). The membranes were hybridized with an *int-2* flanking probe (probe A, refs. 16 and 22), a *neo* probe (probe B, ref. 16) or a *lacZ* probe (probe C, ref. 15). The sizes of the hybridizing fragments are indicated in kb beside each blot. (*Lower*) Restriction maps of the targeted and parental DNAs in the vicinity of the *int-2* locus are shown. Shading of the boxes is as in Fig. 3. Above each map are boxes showing the positions of the probe fragments used in the hybridization analysis and below each map is a schematic depiction of the expected fragments from each enzyme digestion (E, *Eco*RI; H, *Hin*dIII; Xh, *Xho* I; Xm, *Xmn* I). The *Eco*RI sites delimit the endpoints of *int-2* DNA contained in the targeting vector.

entiated cells surrounded by a layer of extraembryonic-like endoderm (17). During this differentiation, *int-2* expression is induced and its RNA is localized in the outer, endodermal, cell layer (12, 14). Due to the low level of *int-2* protein product present in mouse embryos and embryoid bodies, as well as the difficulty of raising high-affinity antibodies directed against undenatured protein, *int-2* protein has not been
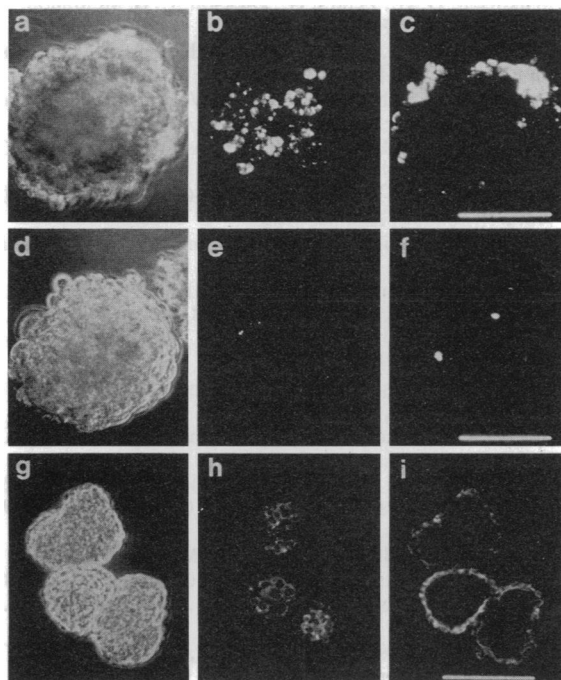

FIG. 5. Fluorescence assay for β-gal activity *in vivo* and immunofluorescent detection of SPARC antigen. Embryoid bodies prepared from 62-8K (*a*, *b*, *c*) and CC1.2 (*d*, *e*, *f*) cells were incubated with FDG (substrate) and fluorescein (product) was detected by using confocal laser scanning microscopy. 62-8K embryoid bodies (*g*, *h*, *i*) were fixed and incubated sequentially with rabbit anti-SPARC serum and donkey anti-rabbit IgG coupled with Texas red. Phase-contrast images are shown on the left (*a*, *d*, *g*). Two fluorescence images in different focal planes are shown for each embryoid body: a section near the surface (*b*, *e*, *h*) and a section 22.5 μm deeper than the first (*c*, *f*, *i*). The section thickness is approximately 7 μm. The scale bars indicate 100 μm.

detected directly in these sources (ref. 24 and unpublished observations).

To determine the pattern of *E. coli* β-gal activity in 62-8K cells as well as in the parental cell line, CC1.2, we prepared undifferentiated cultures and simple embryoid bodies from these cell lines and stained them with 5-bromo-4-chloro-3-indolyl β-D-galactoside (X-Gal), a chromogenic substrate of β-gal (25). Consistent with the low level of *int-2* RNA found in undifferentiated cultures of ES cells (12, 14), very little β-gal activity was detectable in undifferentiated cultures of either cell line (data not shown). In contrast, β-gal activity was readily detectable in embryoid bodies derived from 62-8K cells but not in CC1.2 embryoid bodies (data not shown).

To localize the source of β-gal activity in the embryoid bodies, we stained unfixed 62-8K (Fig. 5 *a*, *b*, and *c*) and control (Fig. 5 *d*, *e*, and *f*) embryoid bodies with a fluorogenic substrate of β-gal, FDG, and examined optical sections of these embryoid bodies for the fluorescent product, fluorescein, using confocal laser scanning microscopy. Fig. 5 shows surface (*b*) and central (*c*) optical sections through a typical 62-8K embryoid body. Only the outer, endodermal, cell layer was labeled, although not every cell in that layer showed activity. *In situ* hybridization to *int-2* RNA in embryoid bodies shows a similarly patchy pattern (12). The control (CC1.2) embryoid bodies were not significantly labeled with FDG. Fig. 5 shows surface (*e*) and central (*f*) sections of a typical CC1.2 embryoid body which had only two or three interior cells that stained positive for β-gal activity. This labeling may reflect endogenous lysosomal β-gal activity in a few disrupted cells.

The endodermal nature of the outer cell layer was confirmed by whole-mount indirect immunofluorescence against SPARC, an endodermal marker (19), followed by confocal laser scanning microscopy. As expected, the labeled cells were confined to the outer surface of the embryoid bodies (Fig. 5 *f* and *g*). Thus the pattern of *int-2–lacZ* expression described above accurately reflects the distribution of normal *int-2* RNA in ES cell-derived embryoid bodies.

DISCUSSION

We have demonstrated that the frequency of gene targeting is not influenced by the length of nonhomologous DNA sequences transferred to the target chromosomal locus. The

size of the heterologous inserts was varied over a range covering three orders of magnitude. As a result of this finding, a wider spectrum of designed genomic alterations is now feasible. Thus, it would be reasonable to attempt substitution of one controlling region of a gene for another, or, as shown here, to replace an entire coding region with another. Also, with respect to homologous recombination, introducing large insertions and generating large deletions are nearly equivalent operations. Therefore, our results suggest that generation of large genomic deletions should also be possible. Overlapping sets of deletions could be used to locate genes within mapping intervals.

Encouraged by our observations on the disruption of the *hprt* gene, we showed that a *lacZ* reporter gene/*neo*ʳ cassette 5.4 kb in length could be efficiently introduced by homologous recombination into the endogenous *int-2* locus. Direct comparison of these results (Table 2) with previously reported results (table 1 of ref. 16) obtained with an *int-2* targeting vector that contained only the *neo*ʳ gene (1.1 kb), shows that the targeted disruption frequencies using these two vectors are essentially equivalent.

Following *in vitro* differentiation, the β-gal activity displayed by cells that contain the fusion construct was consistent with the pattern of *int-2* RNA observed *in situ* by Wilkinson *et al.* (12). *int-2* RNA in the latter study and β-gal activity in this study were up-regulated in endodermal cells. In both cases, not all endodermal cells expressed the gene product in question. Further studies will be necessary to determine whether this result is due to heterogeneity in the *in vitro* produced endoderm as suggested by Wilkinson *et al.* (12). A determination of the relationship between the marker gene's expression and that of *int-2* RNA during actual embryonic development will be feasible when germ-line chimeras that carry the *int-2–lacZ* fusion are produced.

lacZ fusion genes have been introduced as transgenes at random locations within the mouse genome (see for example, ref. 26). Introduction of the *lacZ* reporter gene into endogenous loci by homologous recombination may obviate two serious limitations imposed by the standard transgenic technology. First, homologous recombination places the reporter gene among all of the cis-acting control elements that normally mediate expression of the endogenous gene. Often, the locations of these elements have not been defined or they may be highly dispersed within a locus, making construction of a transgene that mimics the expression of the endogenous gene difficult or impossible. Second, the expression pattern of the reporter gene at the endogenous locus is not subject to the chromosomal position effects that can result from integration of the transgene at ectopic sites. As a consequence of these effects, independent transgenic animals that contain the same *lacZ* fusion construct integrated at different sites may exhibit different patterns of β-gal activity, even when the known cis-acting elements are included in the construct. A consensus expression pattern must be inferred from comparisons of the patterns observed in a number of independent transgenic animals.

As discussed above, the pattern of β-gal activity in heterozygous *int-2–lacZ* mice may provide a sensitive tool for following *int-2* expression in the developing embryo. A unique aspect of this experimental design, which does not apply to conventional transgenes, is that the *lacZ–neo*ʳ cassette inactivates the *int-2* gene. Therefore, homozygous *int-2–lacZ* mice will exhibit the phenotype normally associated with the absence of the *int-2* gene product. As a result, the same cells responsible for the *int-2⁻* phenotype should also be labeled with the *lacZ* gene product. This property may facilitate the interpretation of the resultant phenotype at the cellular level.

lacZ reporter genes have provided an important tool for the analysis of early development in *Drosophila* and *Caenorhabditis elegans* (27–32). Such reporter genes have been particularly instructive in the analyses of interactions among genes that participate in developmental regulatory networks. By moving the recombinant construct into different mutant backgrounds, the effects of other genes on the expression of the fusion gene can be easily assayed. Comparable molecular genetic analysis of mouse development is just beginning. It is our hope that the ability to target reporter genes to loci that mediate developmental decisions will contribute to this emerging analysis.

1. Capecchi, M. R. (1989) *Trends Genet.* **5,** 70–76.
2. Capecchi, M. R. (1989) *Science* **244,** 1288–1292.
3. Rossant, J. & Joyner, A. (1989) *Trends Genet.* **5,** 277–283.
4. Thomas, K. R. & Capecchi, M. R. (1987) *Cell* **51,** 503–512.
5. Bollag, R. J., Waldman, A. S. & Liskay, R. M. (1989) *Annu. Rev. Genet.* **23,** 199–225.
6. Frohman, M. A. & Martin, G. R. (1989) *Cell* **56,** 145–147.
7. Zimmer, A. & Gruss, P. (1989) *Nature (London)* **338,** 150–153.
8. Letsou, A. & Liskay, R. M. (1987) *Genetics* **117,** 759–769.
9. Peters, G., Brookes, S., Smith, R. & Dickson, C. (1983) *Cell* **33,** 369–377.
10. Dickson, C., Smith, R., Brookes, S. & Peters, G. (1984) *Cell* **37,** 529–536.
11. Dickson, C. & Peters, G. (1987) *Nature (London)* **326,** 833.
12. Wilkinson, D. G., Peters, G., Dickson, C. & McMahon, A. P. (1988) *EMBO J.* **7,** 691–695.
13. Wilkinson, D. G., Bhatt, S. & McMahon, A. P. (1989) *Development* **105,** 131–136.
14. Jakobovits, A., Shackelford, G. M., Varmus, H. E. & Martin, G. R. (1986) *Proc. Natl. Acad. Sci. USA* **83,** 7806–7810.
15. Thummel, C. S., Boulet, A. M. & Lipshitz, H. D. (1988) *Gene* **74,** 445–456.
16. Mansour, S. L., Thomas, K. R. & Capecchi, M. R. (1988) *Nature (London)* **336,** 348–352.
17. Martin, G. R., Wiley, L. M. & Damjanov, I. (1977) *Dev. Biol.* **61,** 230–244.
18. Nolan, G. P., Fiering, S., Nicolas, J. F. & Herzenberg, L. A. (1988) *Proc. Natl. Acad. Sci. USA* **85,** 2603–2607.
19. Mason, I. J., Taylor, A., Williams, G., Sage, H. & Hogan, B. L. M. (1986) *EMBO J.* **5,** 1465–1472.
20. Dent, J. A., Polson, A. G. & Klymkowsky, M. W. (1989) *Development* **105,** 61–74.
21. Melton, D. W., Konecki, D. S., Brennand, J. & Caskey, C. T. (1984) *Proc. Natl. Acad. Sci. USA* **81,** 2147–2151.
22. Mansour, S. L. & Martin, G. R. (1988) *EMBO J.* **7,** 2035–2041.
23. Smith, R., Peters, G. & Dickson, C. (1988) *EMBO J.* **7,** 1013–1022.
24. Dixon, M., Deed, R., Acland, P., Moore, R., Whyte, A., Peters, G. & Dickson, C. (1989) *Mol. Cell. Biol.* **9,** 4896–4902.
25. Glaser, R. L., Wolfner, M. F. & Lis, J. T. (1986) *EMBO J.* **5,** 747–754.
26. Goring, D. R., Rossant, J., Clapoff, S., Bratman, M. L. & Tsu, L. C. (1987) *Science* **235,** 456–458.
27. Hiromi, Y. & Gehring, W. J. (1987) *Cell* **50,** 963–974.
28. Driever, W., Thoma, G. & Nusslein-Volhard, C. (1989) *Nature (London)* **340,** 363–367.
29. Goto, R., MacDonald, P. & Maniatis, T. (1989) *Cell* **57,** 413–422.
30. Harding, K., Hoey, T., Warrior, R. & Levine, M. (1989) *EMBO J.* **8,** 1205–1212.
31. Struhl, G., Struhl, K. & MacDonald, P. M. (1989) *Cell* **57,** 1259–1273.
32. Way, J. C. & Chalfie, M. (1989) *Genes Dev.* **3,** 1823–1833.
33. LeMotte, P. K., Kuroiwa, A., Fessler, L. I. & Gehring, W. (1989) *EMBO J.* **8,** 219–227.